AUTOMATIC SEGMENTATION OF COMMON CAROTID ARTERY IN LONGITUDINAL MODE ULTRASOUND IMAGES USING ACTIVE OBLONGS

J. R. Harish Kumar [1, 2], *Kartik Teotia* [2], *P. Kevin Raj* [2], *Jasbon Andrade* [3], *K. V. Rajagopal* [3], *and Chandra Sekhar Seelamantula* [1]

[1]Department of Electrical Engineering, Indian Institute of Science, Bangalore, India
[2] Department of Electrical and Electronics Engineering, Manipal Institute of Technology, Manipal, India
[3] Department of Radiodiagnosis, Kasturba Medical College, MAHE, Manipal, India
E-mail: {harishj, chandrasekhar}@iisc.ac.in, {kartikt4997, kevinyitshak}@gmail.com,
{jasbon.andrade, rajagopal.kv}@manipal.edu

ABSTRACT

We propose a fully automated algorithm for the segmentation of common carotid artery in longitudinal mode ultrasound images using *active oblongs*. The problem of segmentation and subsequent delineation of lumen-intima layer is solved as an optimization of a locally defined contrast function with respect to five degrees-of-freedom that characterize the active oblong. The detection of the common carotid artery and subsequent initialization of the active oblong inside the common carotid artery region has been done using a combination of binary thresholding, Hough transform, and pixel-offset operations. The algorithm has been validated on the Brno university signal processing lab B-mode ultrasound image database, which contains 84 longitudinal mode ultrasound images of the common carotid artery. The segmentation results are validated against the ground truth provided by two practising radiologists using Jaccard and Dice similarity measures. We have achieved a detection and segmentation accuracy of 95.2% and 97.5%, respectively.

Index Terms— Common carotid artery (CCA), segmentation, oblong, Hough transforms, ultrasound (US) images.

1. INTRODUCTION

The common carotid arteries are the main arteries responsible for supplying oxygenated blood to the head and neck. The carotid US imaging is a non-invasive and most commonly performed procedure to detect *stenosis* of the carotid artery, a condition that increases the risk of 'stroke' [1]. A typical carotid artery longitudinal mode US image [2] with manually marked lumen-intima boundary is shown in Fig. 1. Ischemic stroke is the second leading cause of deaths worldwide [3]. It is due to the build up of plaque inside carotid arteries that hampers the blood flow to the brain causing carotid Atherosclerosis disease commonly called stroke [1]. Lifestyle changes and medical treatment can prevent the occurrence of stroke if the disease is detected in early stages. The CCA detection and segmentation in ultrasound images is an imperative step in quantifying the plaque and evaluating the severity of Atherosclerosis causing stroke [4].

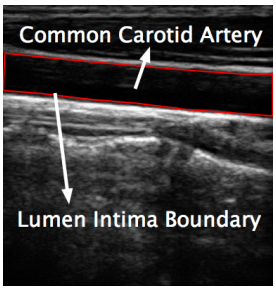

Fig. 1: [Color online] A longitudinal mode ultrasound image with lumen-intima layer manually marked [2].

1.1. Prior Work

A number of studies in the past have addressed the problem of CCA segmentation using transverse mode US images. Mao et al. proposed a semi-automated algorithm based on a deformable active contour model for the segmentation of lumen-intima layer [5]. Hamou et al. proposed a histogram equalization and canny edge detection based segmentation method [6]. Abdel-Dayem et al. proposed a watershed-based algorithm for the segmentation of CCA [7]. Ukwatta et al. proposed a level-set-based semi-automatic algorithm to segment the *media-adventitia* boundary and *lumen-intima* boundary [8]. Hamou et al. used a modified dynamic programming based snake algorithm for solving the CCA segmentation problem [9]. Kumar et al. proposed circular and elliptical active disc-based segmentation techniques for the delineation of media-adventitia and lumen-intima layers, respectively [10], [11]. Since the proposed algorithm addresses the CCA segmentation problem in longitudinal mode US images, it is im-

portant to discuss the prior work done on addressing CCA segmentation in longitudinal mode US images. But, the task of segmentation of CCA using longitudinal mode US images has been addressed by only few researchers. Golemati et al. used Hough transform for segmentation of CCA in longitudinal mode US images [12] . Benes et al. proposed a RANSAC-based method for CCA region localization [13]. Rouco et al. proposed a phase symmetry based CCA detection algorithm for longitudinal mode US images [14]. However, the studies addressing the problem of CCA segmentation in longitudinal mode US images have been conducted on a small number of subjects (4 to 6) [12]. Probably, the dearth of annotated data is the reason for non-reporting of segmentation results/publications on CCA using longitudinal mode US images. To address this problem, a database for measurement of static and dynamic parameters of the CCA in both transverse and longitudinal mode was created and released by a team of researchers at the Brno University Signal Processing Laboratory (SP Lab) [2].

1.2. Our Contribution

The proposed method uses a novel, automated rectangular active contour called '*active oblong*' for the segmentation of CCA due to its inherent capability to segment rectangular-shaped regions. The method is motivated by the technique proposed by Pediredla et al. for the automated image quantitation for western blot analysis [15] and the concept of rectanguscule proposed by Uhlmann et al. [16]. The segmentation procedure consists of two major steps: automatic initialization of the active oblong inside the CCA region using Hough transform and pixel-offset operations and segmentation of the CCA region using active oblong. The oblong use a specified square template called the *mother oblong*, and it evolves to segment the CCA region by a restricted affine transformation. This evolution is achieved through the optimization of the five degrees-of-freedom that parameterize the mother oblong. The energy of the active oblong is defined as the normalized contrast function between the inner rectangle and the region between the outer and inner rectangles. The five free parameters are optimized using the gradient-descent optimizer by minimizing the energy function with respect to each parameter. The proposed method's performance evaluation is done by comparing the results of the proposed technique with the ground truth provided by two expert radiologists for the SP Lab longitudinal mode ultrasound image database [2].

2. ACTIVE OBLONG DESIGN AND OPTIMIZATION

The mother oblong is composed of two concentric rectangles which are aligned with the axes and centered at the origin. The evolution of the oblong is based on a locally defined contrast function defined with respect to five independent degrees-of-freedom out of which two for horizontal and vertical scaling (A and B) , two for translation (x_c and y_c) and one for rotation (θ) of the oblong.

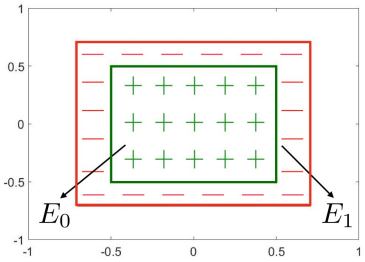

Fig. 2: [Color online] Mother oblong.

2.1. Template Parameterization

The inner square of the mother oblong is parametrized as follows:

$$(x_0(t), y_0(t)) = \begin{cases} \left(t - \frac{1}{2}, -\frac{1}{2}\right); & 0 < t \leq 1 \\ \left(\frac{1}{2}, t - \frac{3}{2}\right); & 1 < t \leq 2 \\ \left(\frac{5}{2} - t, \frac{1}{2}\right); & 2 < t \leq 3 \\ \left(-\frac{1}{2}, \frac{7}{2} - t\right); & 3 < t \leq 4 \end{cases}$$

The outer square is parameterized as:

$$\begin{bmatrix} x_1(t) \\ y_1(t) \end{bmatrix} = \sqrt{2} \begin{bmatrix} x_0(t) \\ y_0(t) \end{bmatrix} \tag{1}$$

where $t \in (0,4]$. The factor $\sqrt{2}$ is to guarantee that the area in the annulus between the two concentric squares is equal to the area of the inner square. A mother oblong template is shown in Fig. 2.

2.2. From Template to Oblong

The mother oblong is parametrized as static, but the offsprings of the mother oblong are active (agile) and are derived from the mother oblong as following:

$$\begin{bmatrix} X_i \\ Y_i \end{bmatrix} = \begin{bmatrix} A\cos\theta & B\sin\theta \\ -A\sin\theta & B\cos\theta \end{bmatrix} \begin{bmatrix} x_i \\ y_i \end{bmatrix} + \begin{bmatrix} x_c \\ y_c \end{bmatrix} \tag{2}$$

for $i = 0, 1$. The oblong's movement is governed by the five free parameters $\{A, B, x_c, y_c, \text{and } \theta\}$.

2.3. Energy Function of the Oblong

We consider the region covered by the inner rectangle as foreground (denoted as τ_0) and that in the annulus between the inner and outer rectangles as the immediate background denoted as $(\tau_1 - \tau_0)$, where τ_1 is the region enclosed by the outer

Table 1: Performance analysis of the proposed method

Algorithm	#Images	Dice index	Jaccard index	Sensitivity	Specificity	Accuracy	Localization
Golemati et al. [12]	4	-	-	0.9375	0.970	0.95375	-
Benes et al. [13]	30	-	-	-	-	-	96.66%
Proposed technique	84	0.9335	0.8722	0.9269	0.9863	0.9750	95.20%

rectangle $(X_1(t), Y_1(t))$ and τ_0 is the region enclosed by the inner rectangle $(X_0(t), Y_0(t))$. The energy of the oblong is defined as the normalized contrast function:

$$\begin{aligned} E &= \frac{1}{AB}\Big(\iint\limits_{\tau_1 \setminus \tau_0} f(X,Y)\,\mathrm{d}X\,\mathrm{d}Y - \iint\limits_{\tau_0} f(X,Y)\,\mathrm{d}X\,\mathrm{d}Y \Big) \\ &= \frac{1}{AB}\Big(\iint\limits_{\tau_1} f(X,Y)\mathrm{d}X\,\mathrm{d}Y - 2\iint\limits_{\tau_0} f(X,Y)\mathrm{d}X\,\mathrm{d}Y \Big) \\ E &= \frac{1}{AB}(E_1 - 2E_0) \end{aligned} \tag{3}$$

The $\sqrt{2}$ factor is to ensure that in regions of constant intensity, the energy E is zero so that the oblong attain a stationary status in such regions. The AB normalization ensures that a tight-fit outline is obtained.

2.4. Optimization

We use the gradient descent technique [17] to optimize the energy E with respect to A, B, x_c, y_c, and θ. The step value γ_n is proportional to the gradient of the function. Starting with an initial guess P_0 for a local minimum of $E[P_0]$ and considering the sequence P_0, P_1, P_2, ... such that,

$$P_{n+1} = P_n - \gamma_n \nabla E[P_n]; \quad E[P_0] \geq E[P_1] \geq E[P_2] ...$$

where P_n denotes the parameter (A, B, x_c, y_c and θ) at iteration 'n'. The gradient descent optimization requires the computation of the partial derivatives of the energy E with respect to the five degrees-of-freedom. We use Green's theorem to achieve optimization in this respect and the final expressions are given below:

$$\frac{\partial E}{\partial A} = \frac{1}{A}\Big(\int_{t\in[1,2]\cup[3,4]} (f(X_1,Y_1) - f(X_0,Y_0))\mathrm{d}t - 2E \Big),$$

$$\frac{\partial E}{\partial B} = \frac{1}{B}\Big(\int_{t\in[0,1]\cup[2,3]} (f(X_1,Y_1) - f(X_0,Y_0))\mathrm{d}t - 2E \Big),$$

$$\begin{aligned} \frac{\partial E}{\partial x_c} = \frac{1}{AB}\Big(&\sqrt{2}\int_1^2 f(X_1,Y_1)\mathrm{d}t - \sqrt{2}\int_3^4 f(X_1,Y_1)\mathrm{d}t \\ &-2\int_1^2 f(X_0,Y_0)\mathrm{d}t + 2\int_3^4 f(X_0,Y_0)\mathrm{d}t \Big), \end{aligned}$$

$$\begin{aligned} \frac{\partial E}{\partial y_c} = -\frac{1}{AB}\Big(&\sqrt{2}\int_0^1 f(X_1,Y_1)\mathrm{d}t - \sqrt{2}\int_2^3 f(X_1,Y_1)\mathrm{d}t \\ &-2\int_0^1 f(X_0,Y_0)\mathrm{d}t + 2\int_2^3 f(X_0,Y_0)\mathrm{d}t \Big), \end{aligned}$$

and

$$\frac{\partial E}{\partial \theta} = \frac{1}{AB}\Big(g(X_1,Y_1) - g(X_0,Y_0) \Big).$$

where,

$$\begin{aligned} g(X,Y) = A^2 &\int_0^1 f(X,Y)\Big(t - \frac{1}{2}\Big)\mathrm{d}t \\ &+ B^2 \int_1^2 f(X,Y)\Big(t - \frac{3}{2}\Big)\mathrm{d}t \\ &+ A^2 \int_2^3 f(X,Y)\Big(t - \frac{5}{2}\Big)\mathrm{d}t \\ &+ B^2 \int_3^4 f(X,Y)\Big(t - \frac{7}{2}\Big)\mathrm{d}t. \end{aligned}$$

3. INITIALIZATION OF THE OBLONG

We perform a hard binary thresholding as a necessary preprocessing step before using the Hough transform algorithm [18] to obtain the boundary separating the lumen-intima and media-adventitia boundary. The binary thresholding value T_v for $f(x,y)$, where, $0 \leq f(x,y) \leq 1$ is arrived at empirically and is set to 0.6 so that the high intensity lumen boundaries are highlighted. This binary intensity thresholding operation results in the preprocessed image $f'(x,y)$. A line can be represented in the form of slope (m) and intercept (c).

$$y = mx + c$$

In the Hough space the line can be represented as a point in the form of ($r \in \mathbf{R}$) and ($\phi \in [0, 180]$).

$$\begin{aligned} r &= x\cos(\phi) + y\sin(\phi) \\ y &= -\frac{\cos(\phi)}{\sin(\phi)}x + \frac{r}{\sin(\phi)} \end{aligned}$$

Using the Hough transform algorithm, the longest line detected in the image $f'(x,y)$ is ultimately the line separating the lumen-intima and media-adventitia layers. The vertical offset midpoint denoted by M_p is obtained to ensure that the oblong is initialized inside the CCA region.

$$M_p = (x_m, y_m \pm S_0)$$

The mid-point of the detected line (x_m,y_m) is offset by S_0 pixels, and here we chose $30 \leq S_0 \leq 50$ pixels. There is

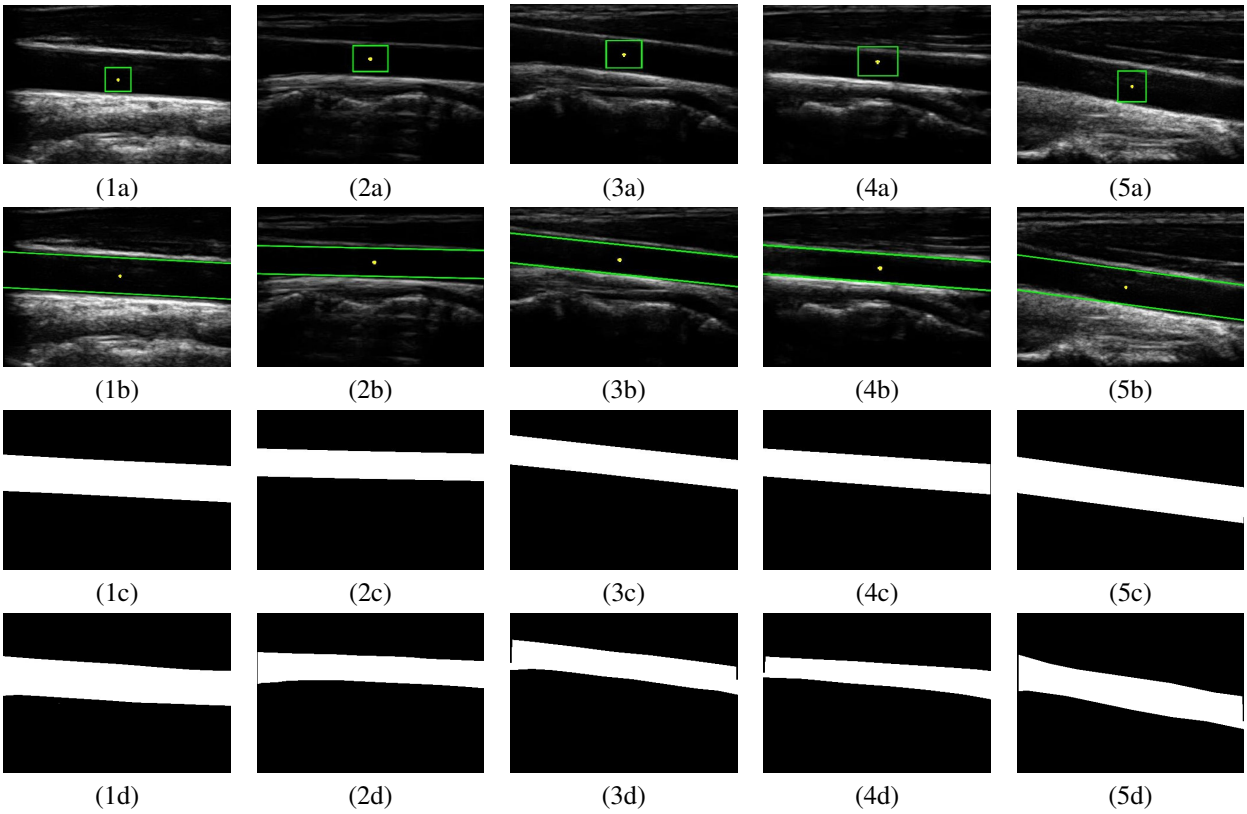

Fig. 3: [Color online] (1a-5a): Input US images with initialization of the active oblong inside the CCA region; (1b-5b): CCA outline by the active oblong; (1c-5c): Segmentation binary map by the proposed method; (1d-5d): Ground truth.

a 'positive' offset if the boundary separating the near wall media-adventitia and near wall lumen-intima is detected, conversely, there is a 'negative' offset if the boundary separating far wall lumen-intima and far wall media-adventitia is detected. The offset sign is automated by calculating the mean pixel intensity both above and below the initialization point by using an $(N \times N)$ window. We chose $N = 60$ and the oblong is initialized in the region where the mean pixel intensity is lower as compared to the other since the CCA region is of low intensity.

4. EXPERIMENTAL RESULTS

The algorithm has been validated on Brno University SP Lab publicly available longitudinal mode US image database [2]. The algorithm is invoked on the binarized US image, we use Otsu's single level thresholding [19] to obtain the binary image. The binarized image is inverted since CCA region is of low intensity and the oblong fits on to bright regions. We have used the Dice index and Jaccard index measure for the purpose of quantitative comparison, the results of which have been shown in Table 1 which also includes the sensitivity, specificity, accuracy, and localization scores. Our method is shown to outperform the existing method which was validated on just four subjects. Figures 3 (1a)-(5a) show the input US images with initialization of the active oblong. Outline and segmentation using the proposed method are shown in Figures 3 (1b)-(5b) and 3 (1c)-(5c), respectively. Figures 3 (1d)-(5d) illustrate the expert ground truth. We could not report the Dice and Jaccard index similarity scores of other methods as their implementations were not publicly available and they had validated their method on only a few number of subjects.

5. CONCLUSIONS

Automated segmentation of CCA is important in evaluating the severity of Atherosclerosis causing stroke. We have proposed a fully automated active oblong based CCA segmentation technique for longitudinal mode ultrasound images. The localization of the oblong is achieved through the Hough transform technique. Optimization of the cost function with respect to five degrees-of-freedom is achieved using the gradient descent technique and Green's theorem. We have evaluated our technique on SP Lab ultrasound image database containing 84 images. The segmentation results with a Dice similarity score of 93.35% demonstrate the reasonable accuracy and robustness of the proposed algorithm.

6. REFERENCES

[1] A. J. Lusis, "Atherosclerosis," *Nature*, vol. 407, pp. 233–241, 2000.

[2] Brno University Signal Processing Laboratory (SP Lab), "Artery database," *http://splab.cz/research/zpracovani-medicinskych-signalu/databaze/artery*.

[3] K. Strong, C. Mathers, and R. Bonita, "Preventing stroke: Saving lives around the world," *The Lancet Neurol.*, vol. 6(2), pp. 182–187, 2007.

[4] I. Shai et al., "Dietary intervention to reverse carotid atherosclerosis," *Epidemiology and Prevention, Circulation*, vol. 121, pp. 1200–1208, 2010.

[5] F. Mao, J. Gill, D. Downey, and A. Fenster, "Segmentation of carotid artery in ultrasound images: Method development and evaluation technique," *Medical Physics*, vol. 27, pp. 1961–1970, 2000.

[6] A. K. Hamou and M. EI-Sakka, "A novel segmentation technique for carotid ultrasound images," in Proc. IEEE Intl. Conf. on Acoustics, Speech, and Signal Processing, 2004, pp. 521–524.

[7] A. R. Abdel-Dayem, M. El-Sakka, and A. Fenster, "Watershed segmentation for carotid artery ultrasound images," in *Proc. 3rd ACS/IEEE Intl. Conf. on Computer Systems and Applications*, 2008, pp. 131–139.

[8] E. Ukwatta, J. Awad, A. D. Ward, D. Buchanan, G. Parraga, and A. Fenster, "Coupled level-set approach to segment carotid arteries from 3d ultrasound images," in *Proc. IEEE Intl. Symposium on Biomedical Imaging*, 2011, pp. 37–40.

[9] S. Osman A. K. Hamou and M. El-Sakka, "Carotid ultrasound segmentation using dp active contours," *Image Analysis and Recognition, Lecture Notes, Springer*, vol. 4663, pp. 961–971, 2007.

[10] J. R. H. Kumar, C. S. Seelamantula, N. S. Narayan, and P. Marziliano, "Automatic segmentation of carotid artery in transverse mode ultrasound images," in *Proc. IEEE Intl. Conf. Image Processing (ICIP)*, 2016, pp. 389–393.

[11] J. R. H. Kumar, C. S. Seelamantula, J. Andrade, and K. V. Rajagopal, "Automatic segmentation of lumen intima layer in transverse mode ultrasound images," in *Proc. IEEE Intl. Conf. Image Processing (ICIP)*, 2018.

[12] S. Golemati, J. Stoitsis, T. Balkizas E. G. Sifakis, and K. S. Nikita, "Using the hough transform to segment ultrasound images of longitudinal and transverse sections of the carotid artery," *Ultrasound in medicine and biology*, vol. 33, pp. 1918–1932, 2007.

[13] R. Benes, M. Hasmanda, and K. Riha, "Object localization in medical images," in *Proc. 34th International Conference on Telecommunications and Signal Processing (TSP)*, 2011, pp. 559–563.

[14] J. Rouco, E. Azevedo, and A. Campilho, "Automatic lumen detection on longitudinal ultrasound b-mode images of the carotid using phase symmetry," *Sensors*, vol. 16(3), pp. s16030350/1–21, 2016.

[15] A. K. Pediredla and C. S. Seelamantula, "Active-contour-based automated image quantitation techniques for western blot analysis," in *Proc. International Symposium on Image and Signal Processing and Analysis (ISPA)*, 2011, pp. 331–336.

[16] V. Uhlmann, R. Delgado-Gonzalo, M. Unser, P. O. Michel, L. Baldi, and F. M. Wurm, "User-friendly image-based segmentation and analysis of chromosomes," in *Proc. IEEE International Symposium on Biomedical Imaging (ISBI)*, 2016, pp. 395–398.

[17] E. K. P. Chong and S. H. Zak, *An Introduction to Optimization*, Wiley-lnterscience, Second Ed., USA, 2001.

[18] R. O. Duda and P. E. Hart, "Use of the hough transformation to detect lines and curves in pictures," *Graphics and Image Processing*, vol. 15, pp. 11–15, 1972.

[19] N. Otsu, "A threshold selection method from gray-level histograms," *IEEE Transactions on Systems, Man, and Cybernetics*, vol. 9, no. 1, pp. 62–66, 1979.